Eur Biophys J (1993) 22:289–300

European Biophysics Journal

Flexoelectric effects in model and native membranes containing ion channels

Alexander G. Petrov*, Barbara A. Miller, Kalina Hristova *, Peter N. R. Usherwood**

Department of Life Science, Nottingham University, University Park, Nottingham NG7 2RD, UK

Received: 14 October 1992 / Accepted in revised form: 25 June 1993

Abstract. An experimental study of flexoelectricity in model membranes containing ion pores and native membranes containing ion channels has been undertaken with the objective of determining the relationship, if any, between flexoelectricity and ion transport. Model membrane patches containing ion pores induced by a blue-green algal toxin, microcystin-LR, and locust muscle membrane patches containing potassium channels were studied using patch-clamp techniques. A correspondence was established between the presence of open channels and pores and the amplitude of the 1st harmonic of the total membrane current when the membranes or patches were subjected to pressure oscillations. The 2nd harmonic of the membrane current provided a measure of the amplitude of a membrane curvature induced by pressure, thus making it possible to determine the membrane flexoelectric coefficient. This study shows that flexoelectricity could be an effective driving force for ion transport through membrane pores and channels, thus further highlighting the possible biological significance of this mechano-electric phenomenon.

Key words: Lipid bilayer membranes – Locust muscle membranes – Patch clamp – Mechano-electric transduction – Flexoelectricity – Ion channels

Introduction

Shortly after the concept of "piezoelectricity" of liquid crystals was introduced (Meyer 1969; later called flexoelectricity by de Gennes 1974) its possible relevance to biomembranes in liquid crystal state was raised (Petrov 1975). Flexoelectricity is a phenomenon of curvature-induced electric polarization of a liquid crystal membrane, in which the molecules of the membrane are uniaxially orientated. Curvature of a membrane bilayer splays the uniaxial orientation of the molecules (lipids, proteins) that it contains and imposes a polar symmetry, such that on one side of the membrane the molecules are moved apart whereas on the other side they are moved closer together. Flexoelectricity results from the resultant electrical polarisation of the membrane. Many native membranes (e.g. those of mitochondria, chloroplasts, erythrocytes, pseudopodia, microvilli, nerve endings, stereocilia, muscle membranes etc.) are known to exhibit changes of curvature. This implies that flexoelectricity is a fundamental biological phenomenon and may be a mechanism for coupling the mechanical and electrical degrees of freedom of a biological membrane (Petrov 1975, 1977, 1978, 1984; Petrov and Bivas 1984).

The existence of flexoelectricity in model (artificial) membranes has been documented experimentally by observing the a.c. displacement currents which accompany pressure-induced periodic variations in the curvature of these membranes. These currents have the same frequency as the membrane oscillations (Petrov and Sokolov 1986; Derzhanski et al. 1981, 1989, 1990). Flexoelectricity has also been reported in patches excised from natural membranes (Petrov et al. 1989). The first indication that flexoelectricity is coupled to transmembrane ion movement was obtained with mechanically-stressed black lipid membranes (BLMs) just prior to their rupture. During this period, metastable, ion-conducting pores were observed and a striking enhancement of the 1st a.c. current harmonic was recorded in the presence of such pores (Petrov and Sokolov 1986). Similar results were later obtained with excised patches of locust muscle membrane (Petrov et al. 1989), i.e. the open states of potassium channels present in such patches greatly increased the amplitude of the 1st harmonic of the total membrane current (I) which was generated by membrane oscillations. A correlation between the conductivity of a BLM and its "piezoelectric response" to pressure has been observed

* *Permanent address:* Biomolecular Layers Department, Institute of Solid State Physics, Bulgarian Academy of Sciences, BG-1784 Sofia, Bulgaria

** *Present address:* Department of Physiology, University College London, Gower Street, London WC1E 6BT, UK

Correspondence to: P. N. R. Usherwood

previously (Passechnik and Bichkova 1978), and was explained in terms of ion currents which are driven through the membrane by pressure. However, this is an unlikely explanation in view of the magnitude of the currents involved (Derzhanski et al. 1981).

In this paper we confirm our previous findings concerning the flexoelectric properties of model and natural membranes (Petrov et al. 1989), and present measurements of the second harmonic of I to estimate the curvature of these membranes. Also, we show that the flexoelectric response is enhanced during the appearance of pores in a model membrane and when ion channels open in a natural membrane.

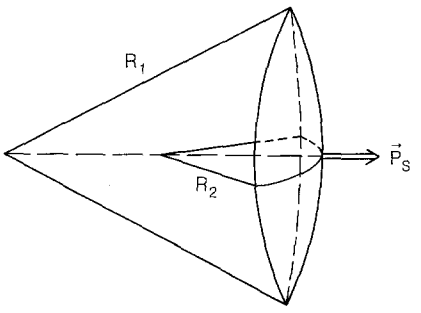

Fig. 1. Schematic representation of curvature-induced polarization of a bilayer membrane. R_1 and R_2 are the two principal radii of curvature at a given point of the curved membrane surface. P_s is the surface polarization at the same point

Theoretical remarks

Phenomenology in flexoelectricity

The basic expression of flexoelectrical theory (Petrov 1975, 1984; Petrov and Bivas 1984) is:

$$P_s = f(1/R_1 + 1/R_2) \quad (1)$$

where P_s is the surface polarization per unit membrane area, R_1 and R_2 are the two principal radii of curvature of the membrane surface (Fig. 1) and f is the flexoelectric coefficient. For a spherically-curved membrane of radius r, Eq. (1) takes the form:

$$P_s = f(2/r). \quad (2)$$

The sign of f is assumed positive if P_s points outwards from the centre of curvature, and negative if it points inwards (Fig. 1). The dimension of f is coulombs, and its expected order of magnitude for zwitterionic lipids with zero charge is 10^{-20} C (Derzhanski et al. 1989). When the surface charge is not zero and the lipid head groups are fully-ionised, f could reach a value of 10^{-18} C; its sign depending upon the sign of the surface charge (Derzhanski et al. 1990).

When a curved membrane with surface polarization P_s, is traversed an electric potential jump U_f is observed which, according to the Helmholtz equation, is:

$$U_f = P_s(\varepsilon\varepsilon_0)^{-1} \quad (3)$$

where ε is the membrane dielectric constant and ε_0 is the absolute dielectric permittivity of free space. This potential change results from differences in the surface potential of the two membrane surfaces due to the curvature (Fig. 2). If the membrane oscillates in time, i.e.:

$$2/r = (2/r_c)\sin\omega t \quad (4)$$

where r_c is the minimal radius of curvature, then the two surface potentials E^{out}_{flexo} and E^{in}_{flexo} will also oscillate; therefore, the latter may be represented as two e.m.f. generators in an equivalent membrane circuit (Fig. 2A). Since they operate in series and in counterphase, they can be combined *algebraically* into one generator. The temporal properties of this lumped e.m.f. depend on whether the membrane has a fixed volume. If there is recruitment of lipid from a reservoir, such as a torus, when a membrane

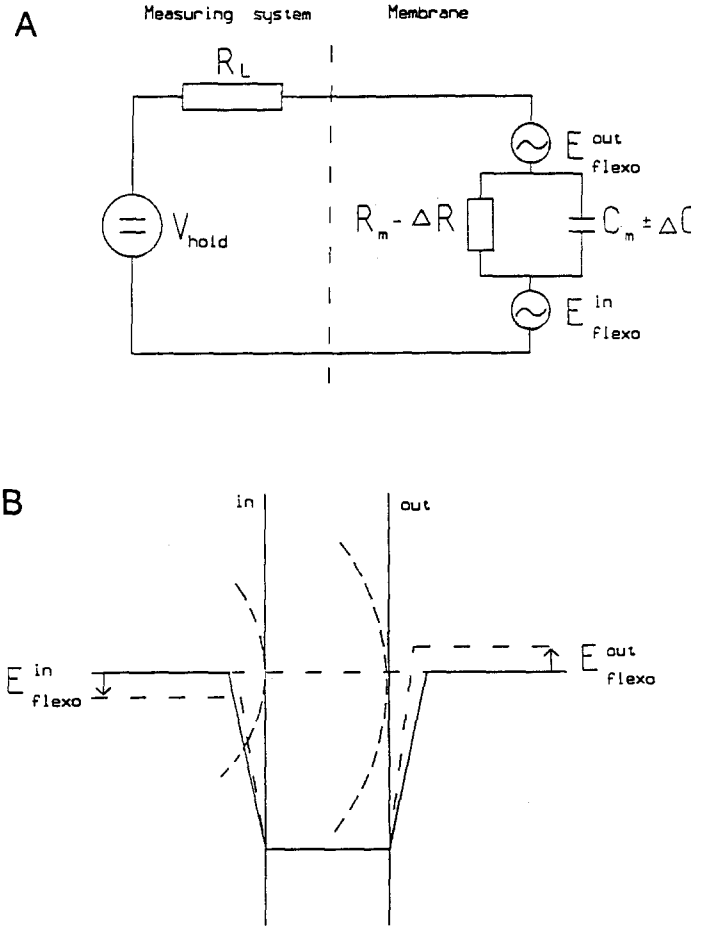

Fig. 2. **A** Equivalent circuit of an oscillating membrane connected to a system (see text) for recording flexoelectricity. V_{hold} is the holding potential of a voltage clamp, R_L is the input resistance of the recording system, C_0 is the membrane capacitance (and ΔC_0 is its variation during oscillatory changes in membrane area), and R_m is the membrane resistance (and ΔR_m is its variation during channel opening). E^{out}_{flexo} and E^{in}_{flexo} are two e.m.f. generators which modulate the surface potentials of the two surfaces of a curved membrane; **B** The case for a positive flexoelectric coefficient, negative surface charge and zero intramembrane field, i.e. zero V_{hold}. Since the two flexoelectric generators operate in counter-phase they can be combined as one generator to produce a potential difference of about 1 mV for a flexoelectric coefficient of 10^{-20} C and for a membrane radius of curvature of 1 μm

is curved by pressure, then the rate of lateral and transverse lipid exchange in the membrane will be limiting. When lipid exchange is prevented or blocked (*B*), changes in membrane polarization and flexoelectric voltage will faithfully follow changes in membrane curvature according to Eq. (1) and (4). The flexoelectric coefficient for *B*, i.e. f^B, can be calculated from these equations. When lipid exchange (*E*) occurs between the membrane and reservoir, there will be a phase shift between the maxima for P_s and that for the membrane curvature, with the amplitude of P_s depending upon the membrane oscillation frequency (Petrov and Sokolov 1986; Derzhanski et al. 1990).

Molecular theory

In the case of *B*, flexoelectrical theory provides an expression for the dipolar (*D*) contribution f^{DB} to f (Derzhanski et al. 1989):

$$f^{DB}=\left[\frac{\mu}{A_0}-\left(\frac{\mathrm{d}\mu}{\mathrm{d}A}\right)_{A_0}\right]d_0 \tag{5}$$

where μ is the normal component of the dipolar moment per lipid head group (considered positive if directed towards the hydrophobic core of a membrane); $\mathrm{d}\mu/\mathrm{d}A$ is its derivative with respect to A, the area per lipid head group; A_0 is the area in a flat membrane, and d_0 is the membrane thickness (strictly speaking, its capacitative thickness). The value ($=f^{DE}$) of f, for the case when lipid exchange occurs freely, is easily obtained from (5) by replacing d_0 with $2\delta_H$, which is twice the distance between the surface of each monolayer, for a membrane comprising uncharged lipids, and the surface of the lipid head groups (Petrov and Bivas 1984; Derzhanski et al. 1989). Using experimentally determined values of μ and $\mathrm{d}\mu/\mathrm{d}A$ for a lecithin monolayer (Paltauf et al. 1971), it can be shown that $f^{DB}=1.10^{-20}$C and $f^{DE}\leq 5.10^{-21}$ C. In the case of a membrane containing lipids with a partial electric charge per head group, βe(where e is the proton electric charge, and β carries the sign of the surface charge and depends on the degree of dissociation of the charged groups), the surface charge contribution of these lipids can also be obtained from (5) by replacing μ with $\beta e\lambda$, where λ is the Debye length when the degree of dissociation β is considered to be area-dependent (Derzhanski et al. 1990).

Flexoelectric potentials, represented by the algebraic sum of $E^{\mathrm{out}}_{\mathrm{flexo}}$ and $E^{\mathrm{in}}_{\mathrm{flexo}}$ (Fig. 2A), are best observed in the absence of an externally-applied potential difference. Therefore, in the case of *B* the transmembrane flexoelectric voltage (U_0) will be (from equations (2), (3) and (4)):

$$U_f=U_0\sin\omega t \tag{6}$$

where $U_0=2f(\varepsilon\varepsilon_0 r_c)^{-1}$. In principle, this voltage could be measured at zero current under current clamp conditions. Alternatively, the current could be measured when the membrane is clamped at zero potential difference (zero V_{hold}). The current (I_f) flowing through the ohmic resistance R_m and capacitive resistance $(\omega C_m)^{-1}$ of the membrane would then be:

$$I_f=(U_0/R_m)\sin\omega t+\omega C_m U_0\cos\omega t \tag{7}$$

i.e. it has an in-phase and a quadrature component with respect to the voltage U_f in equation (6). The amplitude of the first harmonic of the membrane current will be:

$$I_v=(U_0 R_m^{-1})\sqrt{1+(\omega C_m R_m)^2} \tag{8}$$

and can be used for determining f, providing that r_c is known. Equation (7) also gives insight into the influence of channel or pore conductances on f by replacing R_m with $R_m-\Delta R_m$ (or σ_m with $\sigma_m+\Delta\sigma_m$; σ_m being the leak conductance and $\Delta\sigma_m$ being either the open channel conductance or the pore conductance).

Condenser microphone effect

The above considerations only hold when the membrane potential is clamped at zero V_{hold} or, in the case of natural membranes, to a value necessary to compensate for possible differences in the surface potentials of the two faces of the bilayer and to keep the membrane potential field zero and constant. However, when a membrane oscillates and is not clamped at zero V_{hold}, a displacement current I_c is forced to flow through C_m (the membrane capacitance plus the stray capacitance), because capacitance changes with time; viz, $C_0+\Delta C_0\sin^2\omega t$ (where C_0 is the membrane capacitance less the stray capacitance). In other words, the membrane behaves much like a condenser microphone (Ochs and Burton 1974). Consider a membrane which is flat when at rest, and take the time derivative of the charge on C_0, i.e. $Q=C_0 V_{\mathrm{hold}}$ (Petrov and Sokolov 1986). Then:

$$I_c=\omega\Delta C_0 V_{\mathrm{hold}}\sin 2\omega t\,. \tag{9}$$

I_c is a second harmonic with respect to the oscillation frequency and can be used for evaluation of the amplitude of the membrane capacitance change, ΔC_0.

A peculiar feature of membrane patches located at the tips of patch pipettes is that a change in their curvature is inherently related to an area change; i.e. the membrane *must* be stretched in order to be curved. In the case of a membrane with a constant hydrophobic core volume, the relationship between ΔC_0 and area change ΔS_0 is:

$$\Delta C_0/C_0=2\Delta S_0/S_0 \tag{10}$$

where S_0 is the area of "resting" membrane (Wobschall 1971; Szekely and Morash 1980). Using a geometric expression for the area of a spherical cap, the radius of curvature r_c of a membrane patch can be expressed as follows (Petrov and Sokolov 1986):

$$r_c=\frac{1+\dfrac{\Delta C_0}{2C_0}}{\sqrt{\dfrac{\Delta C_0}{2C_0}}}\frac{d}{4} \tag{11}$$

where d is the diameter of the patch.

The driving force for flexoelectriciy is not a change in membrane area *per se*, but a change in membrane curvature. The video images of Sokabe et al. (1991) demonstrate that a membrane patch located at the tip of a pipette is flat at 0 torr pressure and curved in opposite

directions, at +10 torr and −10 torr respectively. Unfortunately, our attempts to visualize membrane patches using simpler techniques were unsuccessful. Nevertheless, we were able to control the geometry of a patch, and to establish patch planarity, by applying a static pressure difference and by employing the "condenser microphone effect" (i.e. by minimizing its first harmonic, as suggested by Ochs and Burton (1974)). If a membrane patch oscillates around a curved state, the variation of its capacitance is not $C_0+\Delta C_0 \sin^2 \omega t$ but $C_0+\Delta C_0 \sin \omega t$. When the membrane is at a non-zero V_{hold}, this is a condition which generates a first harmonic of the capacitance current (Petrov and Sokolov 1986). Experiments with BLMs (Ochs and Burton 1974; Petrov and Sokolov 1986; Derzhanski et al. 1990) have demonstrated that at a non-zero V_{hold} a pre-curved membrane generates a strong first harmonic, and that this is reduced to a minimum when the membrane is brought to a visually flat state.

Identification of flexoelectricity with the first harmonic and the "condenser microphone effect" with the second harmonic is strictly only valid for a membrane oscillating around a flat state. If this condition is not met, then the two phenomena interact. However, even then the flexoelectric component can be distinguished from that due to the "condenser microphone effect" because the latter, unlike the former, is linearly dependent on V_{hold} (see below).

Interaction of flexoelectricity and the condenser microphone effect

When a pre-curved membrane patch is oscillated so that it never achieves a flat position during an oscillation, then the capacitance current I_c will also be a first harmonic (Petrov and Sokolov 1986; Derzhanski et al. 1990):

$$I_c=\omega \Delta C_0 V_{hold} \cos \omega t. \quad (12)$$

The phase of I_c depends on the sign of the capacitance variation ΔC_0, which is related, in turn, to the sign of the pre-curvature: $\Delta C_0>0$ for positive curvature, i.e. the membrane patch is pre-curved outward; $\Delta C_0<0$ for negative curvature. When the sign of the pre-curvature is changed the phase of I_c is altered by 180°.

By combining Eqs. (7) and (12) it can be shown that the quadrature component of I, i.e. I_f+I_c, has an amplitude:

$$\omega(C_m U_0+\Delta C_0 V_{hold}), \quad (13)$$

i.e. it becomes linearly dependent on V_{hold}. The sign of U_0 does not depend on the sign of the pre-curvature, but only on the sign of f (Derzhanski et al. 1990). By comparing the amplitude of I_f at $V_{hold}=0$ and the amplitude of the membrane current when the signs of ΔC_0 and V_{hold} are known, it is possible to obtain the sign of U_0, i.e. the sign of f.

Patches excised from native membranes

The above theoretical comments relate to electrically-symmetrical membranes at zero V_{hold}. With patches excised from native membranes, V_{hold} in (9), (12) and (13) should be replaced by $(V_{hold}+V_{in})$, where V_{in} is the difference between the surface potentials of the two halves of the bilayer (arising from differences in the surface charges and dipolar densities of the two faces of the membrane). Therefore, with inside-out and outside-out patches it is anticipated that opposite signs of V_{hold} will be required for minimization of the amplitudes of second harmonics.

Materials and methods

Patch clamp technique

The patch clamp technique was essentially the same as in a previous study (Petrov et al. 1989). Model membranes were formed at the tips of non-polished patch pipettes from monolayers of diphytanoyl lecithin (DPhL) (Avanti Polar Lipids, Inc., Birmingham, Alabama, USA) using the method of Coronado and Latorre (1983). Typically, 0.3–1 µl of DPhL solution in chloroform or pentane (10 mg ml^{-1}) was spread onto the surface of a KCl buffer solution (150 mM KCl, 10 mM BES, pH 7.0) to form a lipid monolayer. The buffer was contained in petri dishes of 10 cm^2 or 20 cm^2 surface area. Pipettes with large tip openings (3.5–5 µm diam.) were used. Tip diameters were estimated from the pipette resistance (when the pipette was filled with buffer solution and dipped into an identical salt solution) using an experimentally-established correlation between pipette resistance and tip diameter (Sakmann and Neher 1983). It is accepted that this gives only a rough estimate, as the correlation is only valid for a specific tip geometry. Pipettes were pulled from hard borosilicate glass (GC 150-10, Clark Electromedical Instruments, Pangbourne, Reading, U.K.) in two successive pulls using either a vertical puller (Kopf Model 700C, David Kopf Instruments, Tujunga, California) or a horizontal puller (modified Model M1, Industrial Science Associates, Inc. Flushing, NY, USA).

Pores were induced in model bilayers either by prolonged mechanical excitation of the membranes or by the introduction of the blue-green algal toxin, microcystin-LR (MC-LR) (Petrov et al. 1991). The toxin was added as a methanol solution either to the buffer solution in the patch pipette or to the bath, to give a final concentration of 10–20 ng ml^{-1}. MC-LR induces ion-selective pores in DPhL bilayers which exhibit a broad range of conductances. The pores are stress-sensitive (Petrov et al. 1991).

The natural system comprised membrane patches excised from the surface membranes of metathoracic extensor tibiae muscle fibres of adult female locusts (*Schistocerca gregaria*) 7–10 days post-fledging (Huddie et al. 1986; Gorczynska et al. 1993). A muscle was pretreated with collagenase (Sigma 1A, 1–2 mg ml^{-1}) for 1 h at room temperature (20–22 °C) before patch formation. Both the patch pipette and the muscle bath contained standard locust saline (180 mM NaCl, 10 mM KCl, 2 mM $CaCl_2$, 10 mM HEPES, pH 6.8). For all experiments on locust muscle, pipettes were coated with SYLGARD® resin and fire-polished. Tip diameters were c. 1 µm. The resistance of the patch pipettes were determined according to the procedure outlined above. Patches in either cell-attached, inside-out or outside-out configuration were studied.

Mechanical and electrical recordings

The experimental set-up is shown schematically in Fig. 3. A closed pressure system was attached by a plastic tube to the pipette holder by one arm of a T-connection. It was constructed from a small funnel closed by a rubber membrane which, in turn, was connected to a loudspeaker by a plastic rod. Pressure oscillations were generated by feeding the loudspeaker with a sine wave from a function generator (Model 126, Exact Electronic). A reversible peristaltic pump was used to induce static pressure variations. A second plastic tube, identical in dimensions to that of the above closed pressure system, was attached to the other arm of the T-connection. A pressure meter bridge (Fig. 3) attached to this tube provided accurate measurements of pressures in the system. The amplitude of a pressure oscillation at the point of attachment of the pipette to the holder (measured in the absence of a pipette) was attenuated 5-fold at 20 Hz compared to its amplitude at the holder input. This attenuation increased when the oscillation frequency was increased. A further small attenuation occurred in the patch pipette, the size of which depended on the elasticity and tension of the model membrane or natural membrane patch. Therefore, the actual pressure amplitude at the pipette tip was unknown. A direct evaluation of the curvature of a model membrane or natural patch could be obtained using the "condensor microphone effect" (Ochs and Burton 1974; Petrov and Sokolov 1986), i.e. by measuring the 2nd harmonic of the membrane current recorded under voltage clamp (see above).

Electric measurements (see Fig. 3) were undertaken using a patch clamp amplifier (EPC 7, List Electronics) in combination with a dual lock-in amplifier (SR530, Stanford Research Systems) referenced by a function generator (Model 126, Exact Electronic), which in turn excited the loudspeaker. The 1st and the 2nd harmonics of the currents induced by membrane oscillations could be measured separately. A simultaneous display of the rms amplitude and phase of the current was possible. In some cases, the membrane current was recorded together with the driving signal from the generator using a dual channel SONY PCM linked to a standard video recorder. By playing back the current record through the lock-in amplifier referenced by the recorded driving signal, it was possible to measure the 1st and 2nd harmonics from the same data set. To investigate whether the amplitudes of channel or pore currents and the rms amplitudes of 1st harmonic of I were correlated, the recordings were A/D converted and analysed using a Masscomp MC 5500 computer (Mellor et al. 1988).

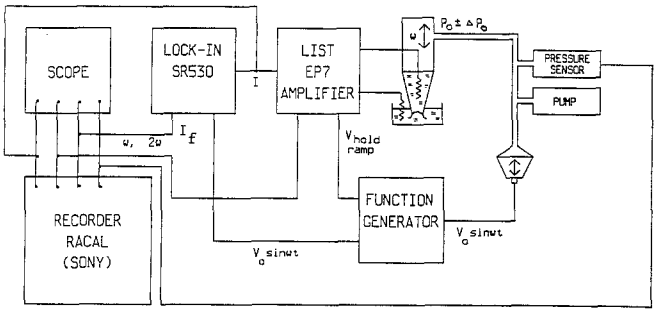

Fig. 3. Schematic diagram of the experimental set-up. Membrane curvature oscillations were excited by a pressure system driven by a loudspeaker, fed by a function generator. Changes in static pressure were produced by a reversible peristaltic pump. Pressure (P_0) was monitored by a pressure meter bridge based on a MPX100AP silicon piezoresistive pressure sensor. Total membrane current was amplified by a patch clamp amplifier connected to a dual lock-in amplifier. Membrane current I, membrane voltage V_{hold}, flexoelectric current (I_f) and pressure were recorded on a 4-channel analog tape recorder. In some cases two of these signals were digitally recorded using a 2-channel PCM linked to a standard video recorder

After forming either a model membrane or a muscle membrane patch, its seal resistance (R_m) was determined using 5 mV rectangular pulses. The slow (C_{slow}) and fast (C_{fast}) components of C_m for model membranes and natural membrane patch were determined using the compensation circuit of the List amplifier.

Mechanical pick-up was minimised by decoupling a membrane or patch preparation from the loudspeaker and by using an anti-vibration air table (Wentworth Laboratories Ltd., Bedford, England). This artefact was examined for each preparation by locating the tip of the patch pipette, without a model membrane or muscle path, just above the surface of the buffer solution or saline. It is noteworthy that under these conditions the pick-up signal never contained a 2nd harmonic. The relative phase of the pick-up was usually set to zero before membrane formation or patching. Consequently, any low amplitude and zero phase signals obtained after forming either a model membrane or locust muscle patch were discarded.

Results

By using a double lock-in amplifier separately to display the amplitude of 1st harmonic of I and its phase, it was possible to ensure that the amplitude of this current was not influenced by phase errors. When a sealed pipette tip was dipped into either saline or buffer solution, the resulting 1st harmonic pick-up was very close, both in amplitude and phase, to that measured when the same pipette tip was in the air just above the saline surface. Therefore, as controls, the amplitude and the phase of the 1st harmonic pick-up in air at the beginning of an experiment were routinely measured. The 1st harmonics of I were at least 10 times larger than the pick-up, and in the presence of open channels or pores they were often 100 times larger. Also their phase was very different from that of controls (see below). 2nd harmonics were never observed under control conditions.

Either model membranes or muscle membrane patches with R_m of 0.5–1 GΩ responded more readily to pressure oscillations than those with higher R_m. Outside-out patches of locust muscle membrane were usually more compliant than either cell-attached or inside-out patches. For some patches of locust muscle membrane with high R_m, it was possible to obtain greater compliance to pressure oscillations by manipulating the static pressure in-

side the pipette, usually by making it more positive (Petrov et al. 1989). For both model membranes and muscle membrane patches it was essential to keep the amplitude of the pressure oscillations as low as possible in order not to excite overtones in the resultant membrane oscillations. These were readily identified as non-zero 2nd harmonics at zero V_{hold}. In fact, it was possible to nullify the 2nd harmonics in inside-out and outside-out patches using V_{hold} positive for outside-out patches and negative for inside-out patches. It is of importance to note that in the studies reported herein, the frequencies of the pressure oscillations that were employed would have greatly limited or precluded an exchange of lipids in the muscle membrane patches of the type described by Sokabe et al. (1991). Therefore, the flexoelectric coefficients that have been obtained are interpreted as corresponding to the *B* situation referred to earlier.

Model membranes without pores and muscle membrane patches not exhibiting channels openings

Figure 4 shows qualitatively typical results for a model membrane which did not contain pores. At $V_{hold} = \pm 100$ mV, the membrane current was clearly modulated by higher harmonics. The simultaneous manifestations of the flexoelectric and "condenser microphone effect" when V_{hold} was not zero is responsible for the difference between the odd and even amplitudes of the 2nd harmonic signal illustrated in this figure. This phenomenon has been observed previously in BLM experiments (cf. Petrov and Sokolov 1986; Fig. 4). The amplitude of the 1st harmonic was dependent on V_{hold}; this could have been due to a slight non-planarity of the membrane (see Discussion). Figure 5 illustrates qualitatively typical results obtained from an outside-out patch of muscle at a time when there were no channel openings. The amplitude of the 2nd harmonic was at a minimum at 5.1 mV and its voltage dependence was very strong, indicating that the amplitude of curvature of the patch was large. The maximum flexoelectric response of this patch was obtained after applying a positive static pressure of 15 torr, which concomitantly resulted in an irreversible decrease of R_m; although the recording in Fig. 5 was obtained after the static pressure was returned to zero. For the model membranes and muscle membrane patches of Figs. 4 and 5 the amplitude of the 1st harmonic was dependent on V_{hold}. In Figs. 6 and 7 the 1st harmonic was independent of V_{hold}, which suggests that in these cases the membranes or membrane patches were initially flat. The data illustrated in Fig. 6 were obtained using frequency pressure oscillations and show that 1st harmonic of I increased in amplitude as the pressure oscillation frequency was raised. This frequency dependence of the amplitude of 1st harmonic of I was investigated over the range 150 to 512 Hz by selecting oscillation frequencies at which the standing wave of sound pressure was maximal at the pipette holder end of the plastic tube. When the pressure amplitude was kept constant, a linear increment of 30 fA(rms) Hz^{-1} was observed. An extrapolation of the relationship between flexoelectric current amplitude and pressure oscillation frequency passed through zero. A similar relationship has been reported for the so-called high frequency regime for generation of flexoelectricity the flexoeletric current in BLMS (Petrov and Sokolov 1986), and represents the capacitive component of I_f (see 2nd term in Eq. (7)).

Figure 7 A illustrates, for a model membrane, the dependence of the rms amplitudes of the 1st and 2nd harmonics (at 20 Hz, in the low frequency regime) on V_{hold}. The envelope of the 2nd harmonic follows closely the theoretical expression in Eq. (9), i.e. it is at a minimum at $V_{hold} = 0$ and increases linearly with V_{hold}. In contrast, the 1st harmonic is essentially voltage-independent, which implies that the membrane was no pre-curved. This permits a reliable evaluation of its flexoelectric coefficient (see below).

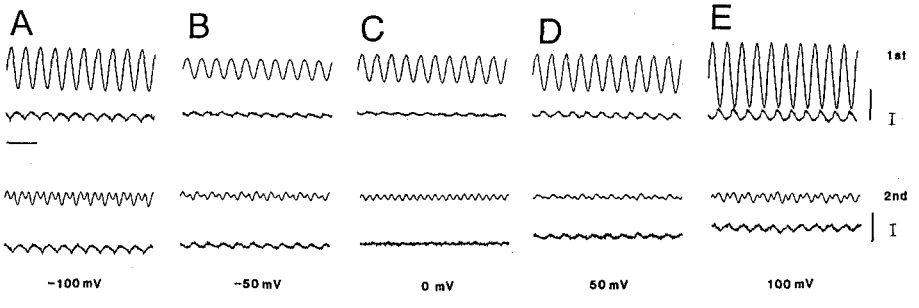

Fig. 4 A–E. Recordings from a pure DPhL membrane (model membrane) using a 150 mM KCl buffer and with pressure oscillations of 20 Hz and 5 torr (pp). **A–E** Upper two traces represent membrane current (*I*; below) and its first harmonic (above; marked 1st) at different V_{hold}; lower two traces represent *I* (below) and its second harmonic (above; marked 2nd) at different V_{hold}. Horizontal bar is 0.1 s; vertical bar is 10 pA for *I* and 1.4 pA for 1st and 2nd harmonics. Current traces were low-pass filtered at 0.5 kHz using a 8-pole Bessel filter. Pipette resistance was 1.4 MΩ. R_m was 1.7 GΩ. The patch capacitance components were $C_{fast} = 2.3$ pF and $C_{slow} = 0.58$ pF. The rms amplitudes of the first harmonic were 577 fA (−100 mV), 316 fA (−50 mV), 400 fA, phase −100° (0 mV), 528 fA (50 mV) 1006 fA (100 mV). The rms amplitudes of the second harmonic were 100 fA (−100 mV), 56 fA (−50 mV) 24 fA (0 mV), 31 fA (50 mV) and 81 fA (100 mV). Controls for mechanical pick-up, established following rupture of the membrane, and with the tip of the patch pipette located out of the saline bath, yielded values of 6.1 fA, phase 10° for the 1st harmonic and negligible values for the 2nd harmonic. These control values were independent of V_{hold}. A flexoelectric coefficient of 5.10^{-20} C is obtained from the above data. The dependence of the 1st harmonic on V_{hold} suggests an inwardly directed curvature of the path and a negative sign for the flexoelectric coefficient or vice vesa (see Discussion). The current traces have a d.c. component, while the 1st and 2nd harmonics are a.c. coupled

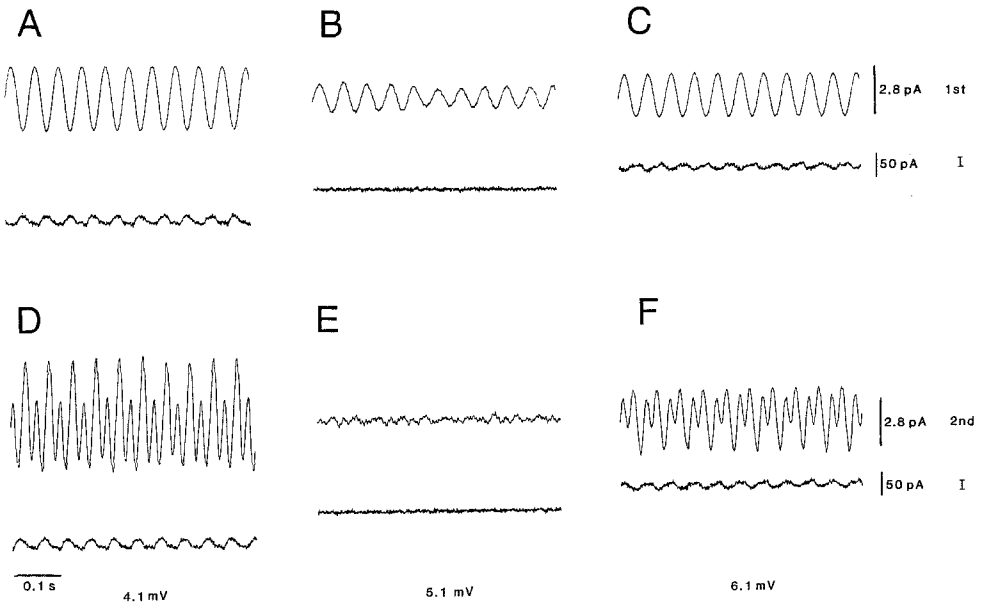

Fig. 5 A–F. Recordings from an outside-out membrane patch excised from locust muscle membrane in standard locust saline. Pipette resistance was 10 MΩ, R_m was 125 MΩ. Pressure oscillations were 20 Hz and 20 torr (pp). Membrane currents (I) (0.5 kHz low-pass filtered) (lower traces in **A–F**) and their 1st and 2nd harmonics (upper traces in **A–C** and **D–F** respectively) at V_{hold} of 5.1 mV, which minimized the 2nd harmonic (*C*), and at ±1 mV with respect to it. The maximum of the 1st harmonic was tuned by first increasing the static pressure of the pipette contents and then releasing the pressure. The rms value of the 1st harmonic was 300 fA, phase 40°, measured at 5.1 mV in the minimum of the 2nd harmonic. Controls with no patch and with the pipette tip out of the saline yielded a 1st harmonic of 60 fA, phase −130° and a 2nd harmonic of 20 fA, phase unstable, with no voltage-dependence, at 60 Hz, 16 torr (pp). Corresponding values for the patch before rupture were: 1st harmonic, 560 fA phase 157° at V_{min}, and 2nd harmonic, 240 fA, phase −23° at $V_{min}+2$ mV. The current traces have a d.c. component, while the 1st and 2nd harmonics are a.c. coupled

Model membranes containing pores and muscle membrane patches containing channels

A strikingly asymmetric flexoelectric response, with respect to the sign of the pipette potential, of a cell-attached patch of locust muscle membrane is illustrated in Fig. 8. With positive V_{hold}, stepwise increases in pipette potential resulted in corresponding changes in amplitude of I_f. This did not happen when V_{hold} was negative. It may be significant that the openings of potassium channels in this patch occurred mainly at positive V_{hold}. The results of this experiment led us to investigate whether there is a correlation between the amplitudes of pore and channel currents *and* the 1st harmonic of I. Figure 7(B–D) illustrates typical responses of the model membrane of Fig. 7A to three successive voltage ramps, recorded at a time when fluctuating pores (induced by long-term mechanical excitation) were present in the bilayer. The simultaneous presentation of I and the rms amplitude of its flexoelectric component (I_f) clearly illustrates that the opening of pores was associated with an increase in the amplitude of I_f. In the absence of pores, a low amplitude (25 fA), voltage-independent 1st harmonic was recorded, whereas during pore openings 1st harmonic responses as large as 30 pA were observed (not shown).

The histograms in Figs. 10A,B and 12A,B are frequency distributions of I amplitudes for a model membrane and a patch of locust muscle membrane respectively. The histograms illustrate either a closed pore or a closed channel state and two open conductance states. Histograms of I_f contain either two peaks or a peak and a shoulder, which are correlated with the closed states and the lower conductance open states present in the pore and channel current histograms (Figs. 10C,D and 12C,D). In principle, there should be two peaks in the histograms of I_f; a peak corresponding to the second open states of Fig. 10A and Fig. 12A was possibly obscured by noise.

Flexoelectricity and ion channels

This relationship was studied most readily in the low frequency pressure oscillation regime where the amplitude of I_f is directly proportional to the membrane conductance. The brief peaks in the flexoelectric response observed at the moment of opening (and closing) of channels in patches of locust muscle membrane and pores in model membranes most probably represent the Fourier component of the channel (or pore) current step at the membrane oscillation frequency. However, there is also a long-term enhancement (10 s to 100 s) of I_f, either during the open state of a channel or during pore opening (Petrov and Sokolov 1986; Petrov et al. 1989) (Figs. 7 and 8). From the histogram in Fig. 10A, it is estimated that the closed state membrane conductance of the model membrane, which was 200±23 pS (determined independently and identified as zero in the histogram), was increased by 60±30 pS (1st open state) and 440±67 pS (2nd open state) respectively when pores occurred.

The histogram of I_f in Fig. 10C gives an estimated rms value of 190±50 fA for I_f, which is characteristic of model membranes without pores. This increased to

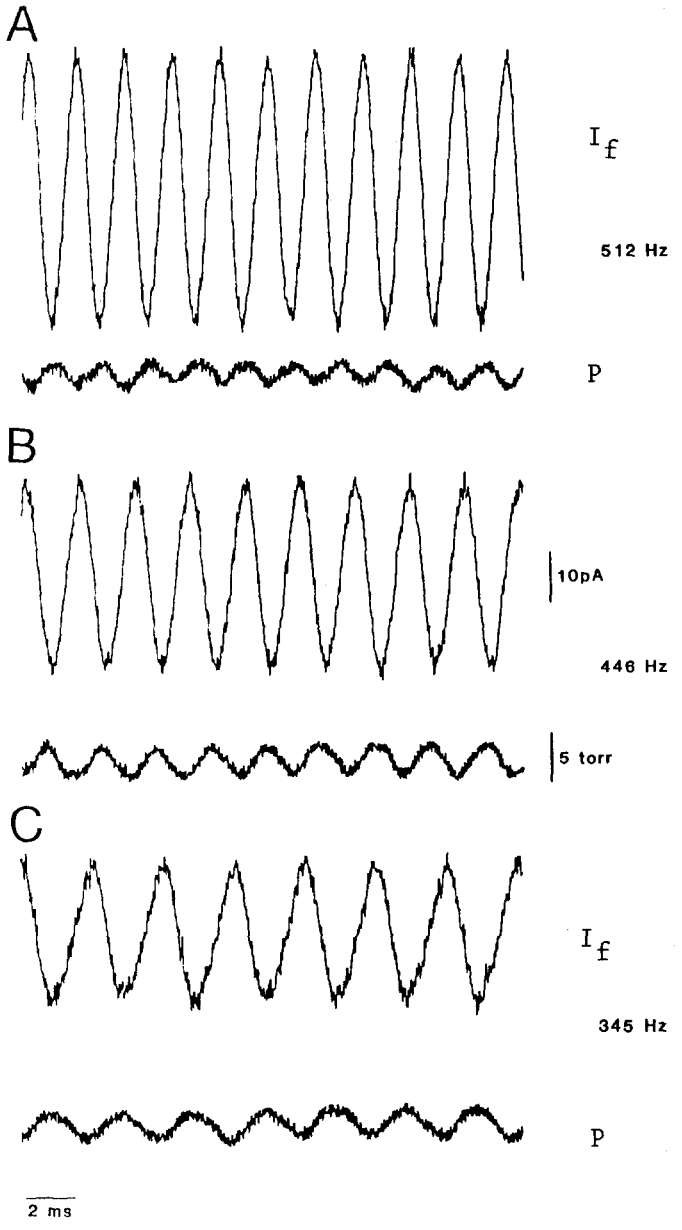

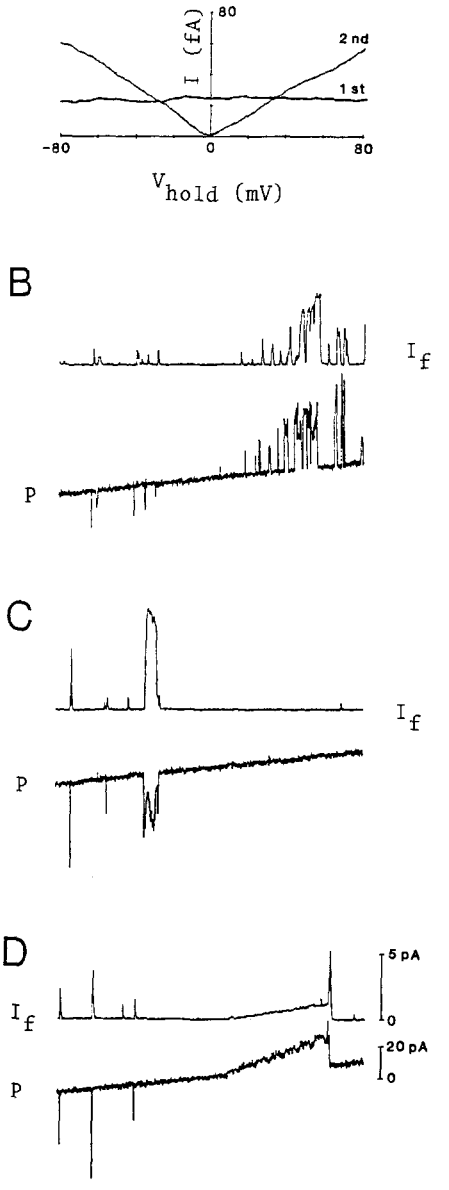

Fig. 6 A–C. Recordings of flexoelectric responses (I_f) from an inside-out patch excised from locust muscle membrane in standard locust saline. Pipette resistance was 6.7 MΩ. R_m was 0.5 GΩ. Patch capacitance components were $C_{fast}=7.5$ pF and $C_{slow}=0.8$ pF. Two types of K^+-channel were present in the patch. **A–C** Upper traces, flexoelectric responses (I_f) at 3 different oscillation frequencies. Lower traces, pressure meter readings (P). Current calibration bar of 10 pA and pressure calibration bar of 5 torr apply to all measurements. I_f were very large, so it was possible to record them directly from the output of a List amplifier. The 1st harmonic was not voltage-dependent. In C at 345 Hz, 2.4 torr (peak-to-peak), a 1st harmonic with a rms amplitude of 9 pA, phase $-72°$ was observed. The control response (not shown) obtained after rupturing the patch and with the pipette tip out of the saline was 0.23 pA, phase 170°

Fig. 7. A–D. Recordings of flexoelectric currents from a model membrane using a 150 mM KCl buffer and 20 Hz, 5 torr (pp) pressure oscillations. Pipette resistance was 1MΩ, R_m was 0.5 GΩ. Capacitance components of the patch were $C_{fast}=2.96$ pF and $C_{slow}=0.88$ pF. A ±80 mV voltage ramp was applied; ramp time was 100 s. A. First (1st) and second (2nd) harmonic of the membrane current (I) showing different dependencies on V_{hold} (±80 mV). The 2nd harmonic follows theoretical predictions (Petrov and Sokolov 1986) by going to zero proportionally to the absolute value of V_{hold}. From the 2nd harmonic the amplitude of the curvature radius was estimated to be 5.2 μm, and from the 1st (voltage-independent) harmonic a flexoelectric coefficient of 4.1×10^{-21} C was evaluated (see text). The membrane did not contain pores. **B–D** Three successive voltage ramps (±80 mV) applied to the same patch as in **A** but when pores were present in the bilayer. The lower traces are membrane currents; the upper traces are the amplitudes of their 1st harmonics. When no pore openings were present, the 1st harmonic was only 25 fA and voltage-indepedent. With pore openings present, flexoelectric responses up to 30 pA in magnitude were observed (not shown). I and the 20 Hz reference signal were recorded during the experiment; subsequently the membrane current was played back through the lock-in amplifier with a 0.1 s time constant in order to obtain its 1st harmonic; the lock-in amplifier was referenced by the 20 Hz signal

340 ± 70 fA during the appearance of a pore. From Eq. (8) the increase in I_f is given by the ratio $(\sigma_m+\Delta\sigma_m)/\sigma_m$. The increase estimated from this equation is 1.3 ± 0.18 times, an estimate which closely matches the experimentally-determined value of 1.79 ± 0.84 times. The correspondence between theoretical and experimental estimates is even

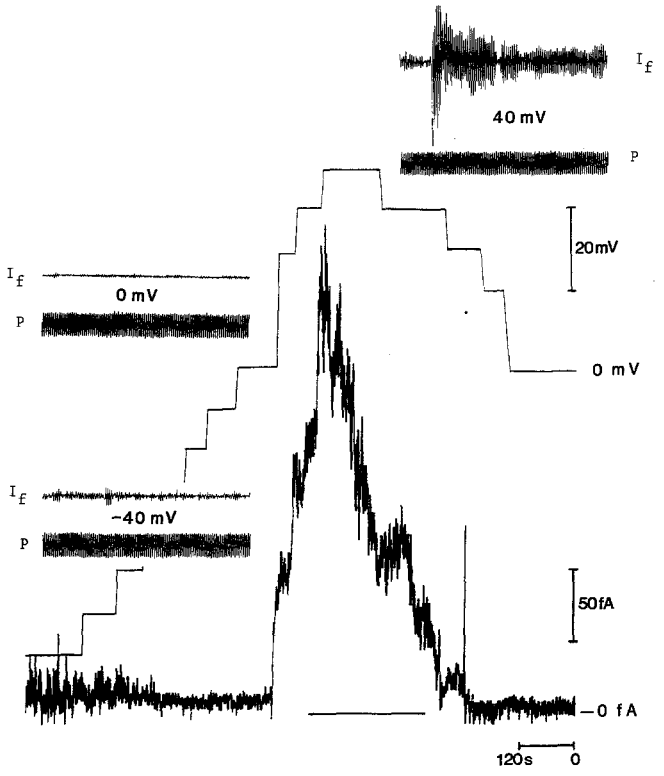

Fig. 8. Recordings of flexoelectric currents (I_f) from a cell-attached patch of locust muscle membrane. The rms amplitude of I_f (*lower trace*) was studied as a function of V_{hold} (*upper trace*) on a slow time scale. (Note that time in this record runs from right to left). 20 Hz, 10 torr (pp) pressure oscillations. Pipette resistance was 9.1 MΩ; R_m was 1 GΩ. Insets show P and I_f as a function of time at V_{hold} of −40 mV (30 fA rms, phase −140°), 0 mV (10 fA rms, phase −73°) and 40 mV (200 to 300 fA rms, phase −56°). Openings of the potassium channels occurred mainly at positive pipette potentials. Because of the relationship between flexoelectricity and channel events, channel openings and closings could be resolved at 40 mV by the marked changes in the amplitude of I. I has a d.c. component, but its 1st harmonic is a.c. coupled

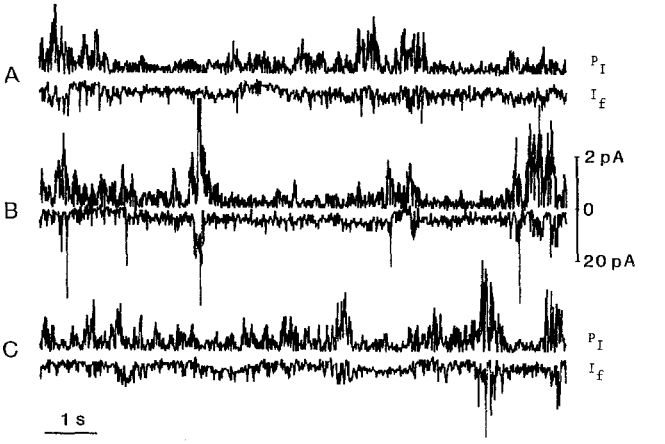

Fig. 9 A–C. Recordings of pore currents (P_I) and rms amplitudes of flexoelectric currents (I_f) obtained from a model membrane containing MC-LR. 20 Hz, 10 torr (pp) pressure oscillation. V_{hold} was −50 mV; R_m was 5 GΩ. The plot demonstrates a correlation between the amplitudes of P_I and the rms amplitudes of I_f. Successive traces of P_I and I_f recorded at −50 mV and low-pass filtered at 3 kHz (P_I, plotted downward following usual convention of negative currents downward; I_f, plotted upward)

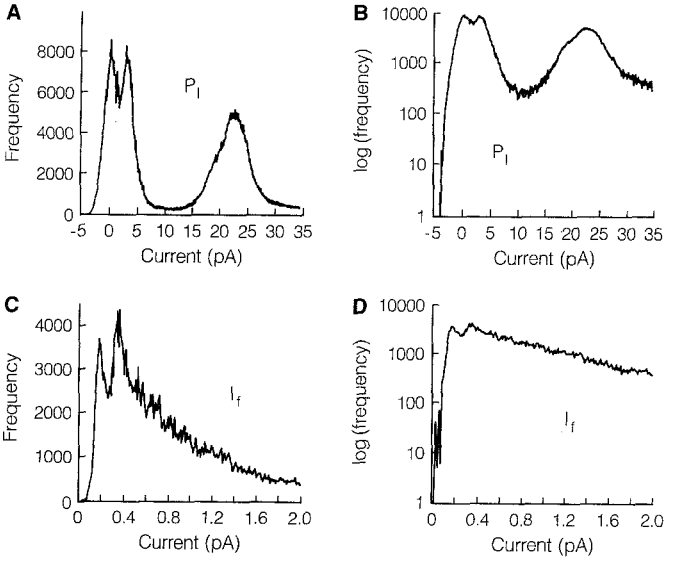

Fig. 10 A–D. Histograms showing frequency distribution of P_I **A–B** and rms I_f **C–D** for the data exemplified in Fig. 7. **A–B** Histograms showing conductances of 60±30 pS and 440±67 pS, at V_{hold} = −50 mV (cf. Fig. 7), which represent the absence and presence, respectively, of pores. Current data were filtered at 3 kHz, sampled at 10 kHz and digitally filtered. Histogram bin width was 0.05 pA. **C–D** Equivalent histogram of I_f showing two clear peaks at 190±50 fA and 340±70 fA. I_f were sampled at 2 kHz and digitally filtered. Histogram bin width was 0.01 pA. The absence of pores in **A–B** is indicated by zero current; I in this state was 10±1.15 pA

better for muscle membrane patches. In Fig. 12A the membrane conductance of 200±7 pS increased by 113±9 pS during channel opening. The theoretical expectation is for an increase in I_f of 1.56±0.06 times; the experimental estimate from the peak and the shoulder in Fig. 12C is 1.41±0.44 times.

Evaluation of the flexoelectric coefficient

This evaluation was based on the 1st and 2nd harmonic response of model membranes with no pores or muscle membrane patches which were not exhibiting channel openings. After determining the resistance of the patch pipette before model membrane or muscle membrane patch formation it was possible to estimate the S_0, d and C_0 of the membrane patch or model membrane using Figs. 2–4 and Figs. 2–8 of Sakmann and Neher (1983). It is accepted that this approach is problematic because of uncertainty over pipette taper *and* over the exact location of a model membrane patch in the tip of the patch pipette. The experimentally-established correlation between pipette conductance and patch capacitance implicitly takes into account the possibility that a patch of locust membrane is located further away from the pipette tip that a model membrane. In the studies described herein, model membranes (but not membrane patches of locust muscle) were always obtained with broad pipettes (see Methods), which reduced errors in the estimation of d and C_0. The

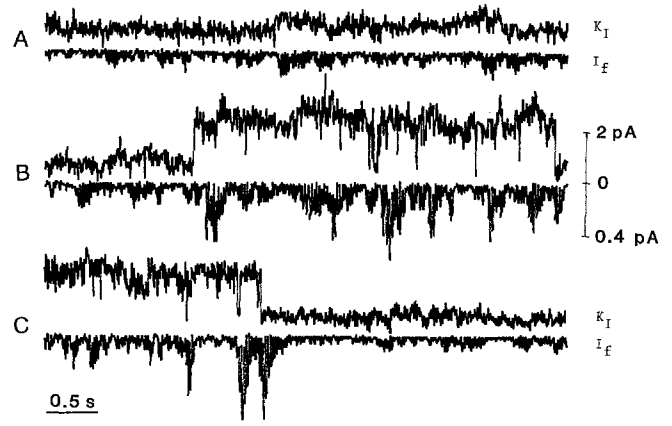

Fig. 11 A–C. Recordings of single K^+-channel currents (K_I) and rms I_f from an inside-out patch excised from locust muscle membrane. Pipette resistance was 6.25 MΩ; V_{hold} was 25 mV; R_m was 5 GΩ. Patch capacitance components were $C_{fast}=4.5$ pF, $C_{slow}=0.08$ pF. 20 Hz 10 torr (pp) pressure oscillations. The plot demonstrates a correlation between the amplitudes of K_I and rms I_f. **A–C** Successive traces of K_I, recorded at $V_{hold}=25$ mV and low-pass filtered at 1 kHz, I_f (downward excursions)

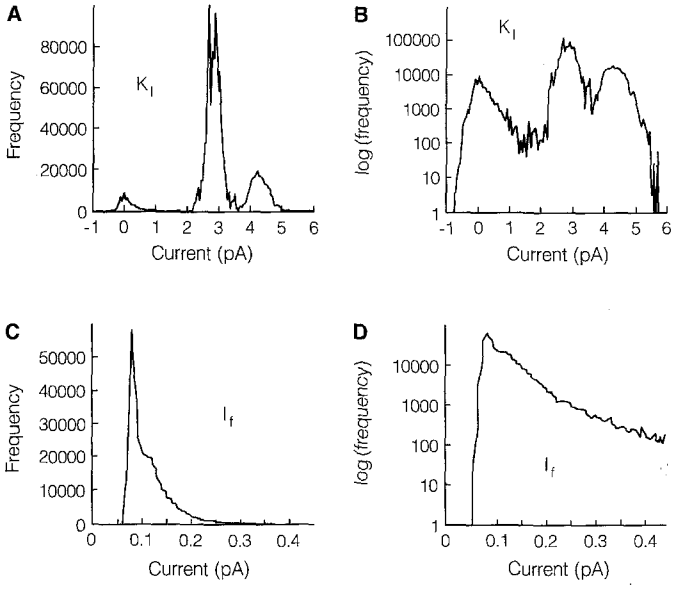

Fig. 12 A–D. Histograms showing frequency distributions of K_I **A–B** and rms I_f **C–D** amplitudes for data exemplified in Fig. 9. **A–B** Current amplitude histograms showing one closed and two open channel conductances 113 ± 9 pS and 169 ± 14 pS, at $V_{hold}=25$ mV; the former is a potassium channel; the identity of the latter was not determined. Current data were low-pass filtered at 1 kHz, sampled at 5 kHz and digitally filtered. Histogram bin width was 0.05 pA. **C–D** Equivalent histograms of I_f showing a peak at 81 ± 12 fA and a shoulder at 115 ± 19 fA. The flexoelectric currents (I_f) were sampled at 2 kHz and digitally filtered. Histogram bin width was 0.005 pA. The closed channel state in **A–B** is indicated by zero current; membrane patch current in this state was 5 pA

2nd harmonic increment ΔI_{2v}, for a given increment of the pipette potential ΔV(with respect to the minimum of I_{2v}) was used to calculate ΔC_0 using Eq. (9). Then r_c, the radius of curvature of the patch, was calculated according to (11). R_m and the capacitance of the membrane patch plus that of the patch pipette ($C_m=C_{fast}+C_{slow}$) were used in estimating f. The stray capacitance of a patch pipette is in parallel with that of a model membrane or membrane patch and also with the R_m. The first harmonic amplitude of I is given by (8). In the low frequency regime, ($\omega<1/R_m C_m$) this current is linearly proportional to the membrane conductance $\sigma_m=1/R_m$. Equations (7) and (8) accommodate the influence of openings of channels or the appearance of pores on I_f by replacing σ_m with $\sigma_m+\Delta\sigma_m$; σ_m being the leak conductance and $\Delta\sigma_m$ being the pore or open channel conductance. In the high frequency regime, ($\omega>1/R_m C_m$) the current is proportional to C_m; it is not sensitive to the conductance changes and tends to grow linearly with the frequency of the pressure oscillations. This behaviour was observed in Fig. 6. The expression for calculating f from the experimental data is:

$$f=\sqrt{2}\,\varepsilon\varepsilon_0\, I_v^{rms}\, R_m.(1+(\omega R_m C_m)^2)^{-1/2}.(r_c/2) \qquad (14)$$

($\sqrt{2}$ was used to convert the measured rms values into amplitudes.)

The estimates for f are summarized in Table 1. The most reliable of these were obtained when the 1st harmonic was voltage-independent, as in Fig. 7A, because under this condition the "capacitance microphone effect" does not influence the 1st harmonic. Values of f for locust muscle membrane patches ($0.8\pm0.4\times10^{-21}$ C from 7 measurements) are lower than those for model membranes ($17.6\pm11\times10^{-21}$ C from 4 measurements). Perhaps this reflects the difference in the diameters of the tips of the pipettes that were used, i.e. they were larger for the model membranes. The model membrane data are in line with the theoretical expectation for lecithin (i.e. $f=5$ to 10×10^{-21} C, Derzhanski et al. 1989). On the other hand, they are strikingly different from results obtained previously for BLMs containing either ethanolamine extracted from *Escherichia coli*, (Petrov and Sokolov 1986) or egg lecithin (Derzhanski et al. 1990; Todorov et al. 1991) which both gave a value for f of about 10^{-18} C. This difference may be related to the complicated visco-elastic properties of the torus of BLMs. A torus would not have been present in the model membrane system described herein. With BLMs, membrane geometry can be monitored with high precision using a holographic interference technique (Picard et al. 1990). By using static pressure to impose a membrane curvature and by observing the sum or the difference of the flexoelectric response and the "condenser microphone effect" (see Theoretical remarks), an unambiguous determination of the sign of f for a BLM can be made.

Following the argument above (Eqs. (12) and (13), it may be concluded that the voltage-dependence of the 1st harmonic in Fig. 4 is consistent either with an inwardly pre-curved membrane and negative f or with an outwardly pre-curved membrane and positive f, the latter being the theoretical prediction for the dipolar contribution of lecithin. However, interpretation of data obtained using patch pipettes is complicated by the fact that in flaccid patches a transmembrane voltage may induce a polarity-dependent curvature of the patch due to the converse flexoelectric effect (Petrov et al. 1989).

When values for R_m were plotted against the calculated values for f in Table 1 only a weak correlation of the

Table 1. Flexoelectric coefficient (f) of diphytanoyl lecithin membranes (DPhL) and locust muscle membrane patches (Lmp), at different frequencies and peak-top-peak amplitudes of oscillating pressure

Membrane	R_{pip} (MΩ)	d (μm)	C_0 (fF)	ΔV (mV)	ΔI_{2v} (fA)	ΔC_0 (fF)	r_c (μm)	I_v (fA)	R_m (GΩ)	C_m (pF)	$f.10^{21}$ (C)
DPhL											
20 Hz, 5 torr	1.36	3.5	100	75	70	10.5	3.8	400	25	2.9	50
DPhL											
20 Hz, 5 torr	1.0	3.9	120	80	60	8.4	5.2	25	8	3.0	4.1[a]
DPhL											
20 Hz, 4 torr	0.74	4.4	150	65	130	22.5	4.0	120	10	2.9	12.8
DPhL											
20 Hz, 4 torr	0.6	5.3	220	10	290	326	2.7	61	2	2.8	3.4
Lmp (inside-out)											
20 Hz, 20 torr	7.7	1.2	12	200	5	0.3	2.8	65	5	5.4	3.2[a]
40 Hz, 20 torr	7.7	1.2	12	20	10	5.6	0.6	75	5	5.4	0.4
Lmp (outside-out)											
20 Hz, 10 torr	10	1.0	8	10	10	11	0.5	25	0.125	6.0	0.02
Lmp (outside-out)											
20 Hz, 10 torr	12.5	0.9	6	70	20	3.2	0.55	130	2.5	7.6	0.86[a]
Lmp (outside-out)											
30 Hz, 10 torr	8.3	1.2	11	10	80	90	0.6	100	0.5	5.8	0.4
Lmp (inside-out)											
20 Hz, 10 torr	6.25	1.4	15	50	2	0.45	2.9	8	5	4.5	0.5
Lmp (cell-attached)											
20 Hz, 10 torr	9.1	1.1	10	40	10	2.8	0.73	10	0.3	8.0	0.03

From the measured pipette resistance (R_{pip}), the pipette tip diameter (d) and membrane patch capacitance (C_0) were roughly estimated using Figs. 2–4 and Figs. 2–6 of Sakmann and Neher (1983). The change in I_c for a given increment of ΔV was measured at the minimum of I_{2v} (or the mean value of ΔI_{2v} for both positive and negative ΔV, if appropriate), and was used to calculate ΔC_0 by (9) and r_c by (11) (see text). When dependent on ΔV, its value at the minimum I_{2v} was used to calculate the flexoelectric coefficient by Eq. (14). R_m and C_m were determined as described in the text. The most reliable data[a] (see Discussion) were obtained when I_v was independent of V_{hold}. Mean value of f for DPhL is 17.6 ± 11.10^{-21} C; for Lmp it is $0.8 \pm 0{,}4 \cdot 10^{-21}$ C. Theoretical predictions for the dipolar contribution of lecithin from (5) are in the range 5 to 10×10^{-21} C

type $f \sim R_m^2$ was obtained. The significance, if any, of this is not understood. If the 1st harmonic effects described herein resulted from pressure-induced ion flow through the membrane seal a correlation of the type $f \sim 1/R_m$ would be expected. Such net ion flow might only take place if the seal is solute-permeable and sufficiently ion selective (see the discussion of pressure-driven currents through membrane defects by Derzhanski et al. 1981). Apart from being very weak, such currents would always be in-phase with the pressure at each oscillation frequency and this relationship would not be influenced by transmembrane voltage. This is obviously not true for the experimental data described herein. Additionally, pressure-driven ion flow could not explain the appearance of a 2nd harmonic under non-zero V_{hold}. Numerous studies with black lipid membranes (Ochs and Burton 1974; Passechnik and Sokolov 1973, Derzhanski et al. 1981, 1989, 1990; Petrov and Sokolov 1986; Todorov et al. 1991) have shown that an oscillating membrane generates both 1st *and* 2nd harmonics.

Discussion

These preliminary results showing increases in the amplitude of I_f which coincide with either channel openings in a natural membrane or the appearance of pores in a model membrane lend support to the hypothesis that flexoelectricity is a possible driving force for ion transport through biological membranes. The data in Fig. 12 show that a rms increase in I_f of 34 fA flows through an open channel or membrane pore, and that during half a cycle of curvature change (2.5 ms) this results in net charge of 0.85×10^{-15} C, i.e. 5312 monovalent ions, being transported through the channel or pore. The direction of transport with respect to the curvature depends on the sign of the flexoelectric coefficient (Petrov 1975, 1977, 1978).

The potassium channels studied herein are stress-activated membrane proteins (Miller et al. 1993), but because their activation pressure thresholds are about 5 torr, it is unlikely that the oscillation and static pressures used in the experiments described herein directly influenced channel gating. The same also holds true for MC-LR pores in model membranes, whose activation pressure threshold is 10–20 torr (Petrov et al. 1991). However, we do not yet have quantitative information on the effect of lateral tension on the open state of these pores and channels. If tension modulation does occur, an appearance of a second harmonic in I would be expected (as in Passechnik and Sokolov 1974; Bogracova et al. 1974; Passechnik 1983), because membrane tension is an even function of membrane curvature according to the Laplace law. The appearance of a first harmonic could only be explained by a substantial initial curvature of the membrane. However, we are convinced this was not the case, at least with the

patch in Fig. 7 which did show a voltage-dependent first harmonic. In future studies we plan to monitor the geometry of the model membrane or natural membrane patch by video microcopy (Sokabe et al. 1991).

In this study we have shown that flexoelectric coefficients of model and natural membranes are closer to theoretical values than has been demonstrated previously. The enhancement of the flexoelectric response seen during channel opening in native membrane patches or in the presence of pores in model membranes supports the hypothesis that flexoelectricity is a driving force for ion transport through membrane channels (Petrov 1975, 1977, 1978; Petrov and Mircevova 1986).

Acknowledgements. We thank Dr. Robert L Ramsey for many helpful discussions. The research reported here was supported by SERC (grant GR/F 15243 to A.G.P. & P.N.R.U.), the British Council (grant to K. H.) and the Bulgarian National Fund "Scientific Studies" (Project F19). We thank Prof. G. A. Codd, Department of Biological Sciences, University of Dundee, Scotland for the sample of microcystin-LR.

References

Bogracova T Ja, Passechnik VI, Sokolov VS (1974) The influence of periodic stretch on the conductivity of modified bilayer lipid membranes. Stud Biophys (Berlin) 42:75–76

Coronado R, Latorre R (1983) Phospholipid bilayers made from monolayers on patch-clamp pipettes. Biophys J 43:231–236

Derzhanski A, Petrov AG, Pavloff YV (1981) Curvature-induced conductive and displacement currents through lipid bilayers. J Phys Lett (Paris) 42:L119–L122

Derzhanski A, Petrov AG, Todorov A (1989) Flexoelectricity of layered and columnar lyotropic phases. Bulg J Phys (Sofia) 16:268–280

Derzhanski A, Petrov AG, Todorov A, Hristova K (1990) Flexoelectricity of lipid bilayers. Liq Cryst 7:439–449

De Gennes PG (1974) The physics of liquid crystals. Clarendon Press. Oxford.

Gorczynska E, Huddie PL, Miller BA, Ramsey RL, Usherwood PNR (1993) Potassium channels of adult locust muscle. (In preparation)

Huddie PL, Ramsey RL, Usherwood PNR (1986) Single potassium channels of adult locust (*Schistocerca gregaria*) muscle recorded using the giga-ohm seal patch-clamp technique. J Physiol 378:60P

Mellor IR, Thomas DH, Sansom MSP (1988) Properties of the ion channels formed by *Staphylococus aureus δ-toxin*. Biochim Biophys Acta 942:280–294

Meyer RB (1969) Piezoelectric effects in liquid crystals. Phys Rev Lett 29:918–922

Miller BA, Petrov AG, Usherwood PNR (1993) Pressure sensitive potassium channels in membrane of adult locust muscle. (In preparation)

Ochs AL, Burton RM (1974) Electrical response to vibration of a lipid bilayer membrane. Biophys J 14:473–489

Paltauf E, Hauser H, Philips MC (1971) Monolayer characteristics of 1,2-diacyl, 1-alkyl-2-acyl and 1,2-dialkyl phospholipids at the air-water interface. Biochim Biophys Acta 249:39–54

Passechnik VI (1983) Viscoelastic properties of biological membrane models and mechanoreception process. D Sc Thesis, Moscow State University

Passechnik VI, Bichkova EJ (1978) Piezoeffect, background conductivity and filtration coefficients of bilayer lipid membranes. Biofizika (Moscow) 23:551–552

Passechnik VI, Sokolov VS (1973) Permeability change of modified bimolecular phospholipid membranes accompanying periodical expansion. Biofizika (Moscow) 18:655–660

Petrov AG (1975) Flexoelectric model for active transport. In: Physical and chemical bases of biological information transfer. Plenum Press, New York London, pp 111–125

Petrov AG (1977) Flexoelectric effects and transport phenomena in biomembranes. Fourth Winter School Biophys. Membrane Transport, Poland. Sch Proc Wroclaw 3:168–176

Petrov AG (1978) Mechanisms of curvature-induced membrane polarization and their influence on some membrane properties. Stud Biophys (Berlin) 74:51–52; Microfische 4:14–25

Petrov AG (1984) Flexoelectricity of lyotropics and membranes. Nuovo Cimento 3D: 174–192

Petrov AG, Bivas I (1984) Elastic and flexoelectric aspects of out-of plane fluctuations in biological and model membranes. Prog Surf Sci 16:389–512

Petrov AG, Mircevova L (1986) Is flexoelectricity the coupling factor between chemical energy and osmotic work in the pump? A model of pump. Gen Physiol Biophys (Bratislava) 5:391–403

Petrov AG, Sokolov VS (1986) Curvature-electric effect in black lipid membranes. Dynamic characteristics. Eur Biophys J 13:139–155

Petrov AG, Ramsey RL, Usherwood PNR (1989) Curvature-electric effects in artificial and natural membranes studied using patch-clamp techniques. Eur Biophys J 17:13–17

Petrov AG, Ramsey RL, Codd GA, Usherwood PNR (1991) Modelling mechanosensitivity in membranes: effects of lateral tension on ionic pores in a microcystin toxin-containing membrane. Eur Biophys J 20:17–29

Picard G, Schneider-Henriquez JE, Fendler JH (1990) Holographic interferometry of ultrasmall-pressure-induced curvature changes of bilayer lipid membranes. J Phys Chem 94:510–513

Sakmann B, Neher E (1983) Geometric parameters of pipettes and membrane patches. In: Sakmann B, Neher E (eds). Single channel recording (eds). Plenum Press, New York London, pp 37–52

Sokabe M, Sachs F, Jing Z (1991) Quantitative video microscopy of patch clamped membranes: stress, strain, capacitance and stretch channel activation. Biophys J 59:722–728

Szekely JG, Morash BD (1980) The effect of temperature on capacitance changes in an oscillating model membrane. Biochim Biophys Acta 599:73–80

Todorov AT, Petrov AG, Brandt MO, Fendler JH (1991) Electrical and real-time stroboscope interferometric measurements of bilayer lipid membrane flexoelectricity. Langmuir 7:3127–3137

Wobschall D (1971) Bilayer membrane elasticity and dynamic response. J Colloid Interface Sci 36:385–396